AD-A047 192 MICHIGAN TECHNOLOGICAL UNIV HOUGHTON DEPT OF METALLU--ETC F/G 11/6
CAVITATION-INDUCED EROSION OF TI-6AL-4V.(U)
OCT 77 D ESSENMACHER, M F PREZKOP N00014-76-C-0037

UNCLASSIFIED TR-8 NL

END
DATE FILMED
1 -78
DDC

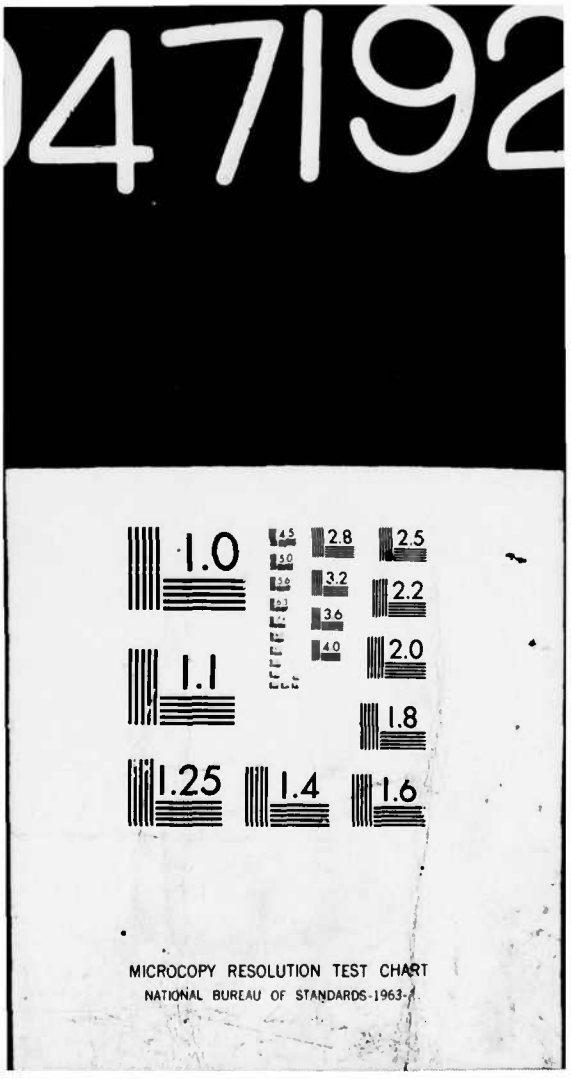
47192
1.0
1.1
1.25
1.4
1.6
1.8
2.0
2.2
2.5
2.8
3.2
3.6
4.0
MICROCOPY RESOLUTION TEST CHART
NATIONAL BUREAU OF STANDARDS-1963-A

(12) U.S.

TECHNICAL REPORT No. 8

To

THE OFFICE OF NAVAL RESEARCH

CONTRACT No. N00014-76-C-0037

# CAVITATION-INDUCED EROSION OF Ti-6Al-4V



BY

D. ESSENMACHER, M. F. PREZKOP, D. E. MIKKOLA AND D. A. KOSS

DEPARTMENT OF METALLURGICAL ENGINEERING
MICHIGAN TECHNOLOGICAL UNIVERSITY
HOUGHTON, MICHIGAN U.S.A.

# Cavitation-Induced Erosion of Ti-6Al-4V

D. Essenmacher,* M. F. Prezkop,** D. E. Mikkola and D. A. Koss
Department of Metallurgical Engineering
Michigan Technological University
Houghton, MI 49931

## Abstract

Cavitation-induced erosion has been examined in Ti-6Al-4V in the mill annealed, solution-treat-and-aged, and beta annealed conditions. Weight-loss data show only small differences between heat treatments with the solution-treat-and-aged microstructure exhibiting the lowest weight loss rates. Sequential micrographs of the same specimen area as a function of erosion time show that initially fracture occurs along the $\alpha$-$\beta$ interfaces and along crystallographic slip bands in the $\alpha$-phase. The early stages of erosion are also dependent on the orientation of the Widmanstatten colonies in the beta annealed condition. These observations strongly suggest that fatigue fracture is important, at least in the early stages of the cavitation erosion process. Depression of the softer $\alpha$-phase also occurs at short exposure times, and this leads to fracture and removal of the exposed phase; i.e., $\beta$ or tempered martensite. However, examination of the eroded surfaces in the later stages where considerable material has been removed shows no evidence of the underlying microstructure, despite the distinct differences in the microstructures of the samples tested.

*presently with Hamill Mfg. Co., Washington, MI 48094
**presently with General Motors Corp., Defiance, OH 43512

(See 1473)

## Introduction

The erosion of alloys by cavitation has received considerable attention in recent years. Much of this effort has been directed toward examining and correlating weight loss data with various mechanical properties. As a result, based primarily on macroscopic observations, many theories and rationalizations have emerged to account for cavitation-induced erosion. In an effort to understand the cavitation erosion process, the present study reports observations of cavitation-induced erosion as this process relates to alloy microstructure and metal removal on a microscopic scale. There have been previous studies relating erosion behavior to microstructure. For example, the cavitation-induced erosion of a pure Aℓ[1] and a single phase Cu-Au alloy[2] have been examined in detail as has the influence of a cavitation-induced phase transformation on the erosion process in a Co-base alloy.[3] Some observations of the early stages of erosion in a number of alloys have also been presented.[4] However, there has been essentially no systematic study of the sequence of the metal removal process during cavitation-induced erosion of a multiphase alloy in which the nature and morphology of the phases present have been controlled by heat treatment. The present research attempts to identify the sequential relationships between cavitation-induced erosion, microstructure, and metal removal during the cavitation process utilizing an α(hcp)-β(bcc) Ti-6Aℓ-4V alloy as a model system. This alloy is attractive for the present study in that it is well characterized from both microstructural and mechanical behavior standpoints[5-8] and can be easily heat-treated to several distinct and yet commercially common microstructures.

## Experimental Procedure

The Ti-6Aℓ-3.9V (.14% oxygen) used for this study was initially in the form of one-inch thick plate in the mill-annealed (MA) condition. As mill-annealed, the alloy had an α-β microstructure consisting of 88% α-phase somewhat elongated along and transverse to the rolling direction. Erosion studies were performed on 1.9 x 3.2 x 0.25 cm specimens cut from the face perpendicular to the rolling direction, in which case the microstructure appears as in Fig. 1. In addition, a beta annealed (BA) microstructure was obtained by heat-treating in vacuum at 1025°C for 30 min., furnace cooling to 920°C for 20 min. followed by 2 hours at 705°C, and finally air cooling to room temperature. The resulting BA microstructure is shown in Fig. 1 and consists of colonies of alternating Widmanstatten α and β plates with a volume fraction of the α-phase (∿84%) nearly equal to that in the MA condition. Finally, a third microstructure consisting of equiaxed primary α (∿40%) + tempered martensite (see Fig. 1) was produced by a solution-treat-and-age (STA) heat treatment. This consisted of heat treating in vacuum at 950°C for ½ hr., water quenching and then aging at 500°C for 8 hours to temper the martensite which formed upon quenching.[7,8] The corresponding yield strengths and hardnesses are noted in the caption to Fig. 1.

Cavitation was induced by placing the sample 0.61mm from a 1 $cm^2$ Ti-tipped exponential horn oscillating at 20 kHz with a peak-to-peak amplitude of ∿0.12mm. All of the tests were performed in distilled water at a temperature of ∿14°C.

The samples were exposed to cavitation for various time intervals (up to fourteen hours total in increments of 2 to 15 minutes), removed, weighed, and examined by scanning electron microscopy. Vickers hardness indentations were used to locate selected areas with the microscope so that the erosion process could be observed sequentially for a specific region on the surface.

## Experimental Results

The weight-loss data (see Fig. 2) show only small differences between the heat treatments with the STA microstructure exhibiting the lowest weight-loss rates. The weight-loss curves in Fig. 2 are characterized by a well-defined incubation period (up to ∿2 hrs.) as a "steady state" zone beginning at about four hours exposure time. As is commonly observed, the data show considerable experimental scatter, possibly due to random removal of very large fragments of material. The straight line drawn through the "steady state" data in Fig. 2 indicates the statistical mean of the weight-loss rate for this period (4-14 hours). Comparison of these data to previously published for cavitation erosion of Ti-6Aℓ-4V[9] is difficult because of differences in experimental techniques and the fact that the microstructural conditions were not specified in the previous measurements. As will be noted later, some aspects of the rain erosion behavior of Ti-6Aℓ-4V[10] are similar to the observations reported here.

The erosion process can be examined most effectively by observing a specific region of the eroding surface sequentially as a function of time. Therefore, a series of sequential micrographs were obtained for each heat treatment and of these the early stages of the erosion process, from the incubation period to beginning of the "steady state" stage, are particularly informative. Examples of these micrographs are shown in Figs. 3, 4, and 6.

Both the BA and MA samples exhibit obvious similarities in their response to cavitation-induced erosion and may be considered together (see Fig. 2 and compare Figs. 3 and 4). After exposures of ∿5 min., all of the specimens showed a depression of the α-phase leaving the β-phase or tempered martensite in relief. Close examination of Figs. 3 and 4 shows that the development of surface relief is followed by a localized fracture process in which fracture

occurs predominantly along crystallographic planes in the α-phase matrix as well as within the β phase and/or along the α-β interfaces. Fracture along crystallographic planes which intersect the β plates is demonstrated in Fig. 3 in which faintly visible slip bands along well-defined crystallographic planes marked S are formed by 1/2 hr. and these lead to local fracture along the plane by 2 hours. Inspection of Fig. 3 at 2 and 2.5 hrs. indicates that local fracture has occurred along many such slip bands, most being parallel and belonging to the same general slip system. Fig. 4 shows the same type of fracture process developing from slip lines in the α-phase of the MA condition at 1.5 and 2.0 hrs.

The other dominant path for local fracture in MA and BA microstructures occurs in connection with the β phase, particularly along the α-β interface, as is illustrated at 2 hrs. in Fig. 3 and the 1-1/2 and 2 hr. states in Fig. 4. While it appears that this fracture occurs predominantly along the α-β interface, there is evidence for fracture within the β-phase. This type of fracture and removal of the β-phase has also been observed during rain erosion of the alloy.[10] Careful examination of Figs. 3 and 4 indicates that the fractures along crystallographic planes in the α-phase are usually associated with regions of interface fracture. Although it appears that the crystallographic cracking of the α-phase occurs after the interface fracture, further work will be necessary to establish the exact sequence.

It should be noted that in the BA condition, the transition from the incubation period to the "steady state" stage is sensitive to colony orientation, as is shown in Fig. 5. Of the four colonies shown in Fig. 5, one clearly is comparable to the 1 hr. case in Fig. 3 while others are similar to a more eroded version of the area shown in Fig. 3 for 2-1/2 hrs.

The STA condition responds to the early stages of cavitation-induced erosion somewhat differently than the MA and BA samples. Fig. 6 shows that during the

incubation stage, cavitation causes obvious depression of the primary α-phase thereby exposing the interface between the tempered martensite and the primary α. While slip lines and small crystallographic cracks are visible in the α-phase, most of the initial fracture occurs along the α-tempered martensite interfaces; see the 2 and 3 hr. cases in Fig. 6. At longer times corresponding to the beginning of the steady state region (3-4 hours), fracture becomes pronounced along crystallographic planes in the primary α-phase (see Fig. 6), and this is important in the removal of the primary α-phase. The cracks that form within the tempered martensite appear to reflect the plate-like morphology of the martensite which formed prior to tempering (see Fig. 1),probably with the fracture path following the plate interfaces.

Once steady-state cavitation erosion is fully attained, the appearance of the eroding surfaces no longer changes perceptibly with time and the topographies are as shown in Fig. 7. An interesting aspect of this observation is that the eroded surfaces during the steady-state stage show essentially no evidence of the underlying microstructure. This stage of the cavitation erosion process is characterized by substantial undercutting and removal of chunks of metal.

## Discussion

It is clear from the scanning electron micrographs of the eroding surfaces that basic fracture processes play an important role in cavitation-induced erosion of Ti-6Al-4V. Certain aspects of the fracture events, at least in the early stages of this process, have obvious similarities to fatigue cracking in α-β Ti alloys. For example, Stage I crystallographic fatigue cracking across primary α or α-β colonies is well-known in Ti alloys;[11-15] such cracking occurs on the basal plane or on a plane ∿15° from the basal plane[16] and the ease of this form of crack propagation is very sensitive to colony orientation in an

α-β Ti alloy.[17] These results are consistent with the present observations of crystallographic cracking within the α-phase and across α-β lamellae as well as the dependence on α-β colony orientation in Figure 5. In particular, slip lines form initially in the α-phase at short exposure times and these develop subsequently into observable cracks which grow as a function of time; this is characteristic of a Stage I fatigue fracture process. Such crystallographic fatigue cracking in α-β Ti alloys is characterized by a flat, cleavage-like fracture surface[13,14,16,17] which is similar to the slip band cracks in the present study. Fatigue of α-β Ti alloys is also characterized by fracture along α-β interfaces,[11,12,14] and this is a common fracture path in the present study. Thus we conclude that there is evidence strongly suggesting fatigue fracture is important in the early stages of cavitation-induced erosion of these alloys.

Since the scale of the microstructure exceeds that of the metal particles being removed, both α-β interface cracking and fracture across the α-phase must occur. This behavior is established during the incubation period prior to the steady-state stage of erosion. Because there is no evidence of the underlying microstructure in the final stage of erosion, it is difficult to interpret the small, but relatively distinct differences in erosion rates between the heat treatments in Figure 2. Nevertheless, it appears that the lower final erosion rate of the STA microstructure must be related to a greater resistance to fracture initiation. If the data on which Fig. 2 is based are examined more closely, there is evidence for delayed fracture initiation in the STA specimen. Taking the time interval necessary for removal of 1 mg of material as a more definite incubation time gives the following: MA - 217 min., BA - 214 min., and STA - 240 min. Therefore, fracture initiation in the STA condition is more difficult as might be expected from both the presence of the tempered martensite

phase and the mechanical properties. Also, it should be noted that quantitative metallography showed the surface to volume ratio of interphase boundary to be the least in the STA specimen.

Tensile stresses are normally associated with the fracture process described above. In the steady-state stage, the presence of such stresses can result simply from the collapse of cavities in the "undercut" regions of the metal surface. The resulting bending moments give rise to the tensile stresses required for the fracture during this stage. The same reasoning can be applied to the incubation period of cavitation in which deformation-induced depression of the softer $\alpha$-phase exposes the $\alpha/\beta$ or $\alpha$/tempered martensite interface to the undercutting process; this is especially evident in the STA condition. At least small tensile stresses must also be present to cause fracture along slip bands on an otherwise relatively smooth region of the surface, as in Fig. 3. The origin of these stresses is not clear.

## Summary

Cavitation-induced erosion in Ti-6Al-4V is a fracture process involving cracking along slip bands in the $\alpha$-phase and long $\alpha$-$\beta$ or $\alpha$-tempered martensite interfaces. While local fracture in the incubation period follows microstructural features and is sensitive to microstructure, the eroded surface in the steady-state stage shows no evidence of the underlying microstructure. The experimental observations strongly suggest that fatigue fracture processes are involved in both initial material damage and in eventual material removal.

## Acknowledgements

The authors would like to thank Mr. E. T. Puuri for technical assistance. This program was supported by the Office of Naval Research through Contract No. N00014-76-C-0037.

## References


1. B. Vyas and C. M. Preece, in Erosion, Wear, and Interfaces with Corrosion, ASTM STP 567, ASTM, Philadelphia, 1973, p. 77.

2. R. N. Wright and D. E. Mikkola, Mat. Sci. Eng., 26 (1976) 263.

3. D. A. Woodford, Metall. Trans., 3 (1972) 1137.

4. C. M. Preece, S. Dakshinamoorthy, S. Prasad, and B. Vyas, Proc. 4th Int. Conf. on the Strength of Metals and Alloys, Vol. III, p. 1397, ed. Laboratoire de Physique du Solide, I.N.P.L., Nancy, France (1976).

5. P. J. Fopiano, M. B. Bever, and B. L. Averbach, Trans. ASM, 62 (1969) 324.

6. P. J. Fopiano and C. F. Hickey, Jr., J. Testing and Eval., 1 (1973) 514.

7. D. J. Maykuth, R. E. Monroe, R. J. Favor, and D. P. Moon, Ti-6Al-4V Handbook (Processes and Properties Handbook), DMIC Publication (1971).

8. G. Welsch, G. Lutjering, K. Gazioglu, and W. Bunk, Met. Trans. 8A (1977) 169.

9. G. C. Gould, in Characterization and Determination of Erosion Resistance, ASTM STP 474, ASTM, Philadelphia, 1970, p. 182.

10. W. F. Adler and R. F. Vyhnal, Proc. 4th Int. Conf. on Rain Erosion and Assoc. Phenomena, Meersburg, Germany, (1974).

11. C. H. Wells and C. D. Sullivan, Trans. ASM 62 (1969) 263.

12. D. K. Benson, J. C. Grosskreutz, and C. G. Shaw, Met. Trans. 3 (1972) 1239.

13. P. E. Irving and C. J. Reevers, Mat'l Sci. and Eng. 14 (1974) 229.

14. C. A. Stubbington and A. W. Bowen, J. Mat'ls. Sci. 9 (1974) 941.

15. G. R. Yoder, L. A. Cooley, and T. W. Crooker, NRL Report 8048, Nov., 1976.

16. D. A. Meyn, Met. Trans. 2, (1971) 853.

17. C. C. Wojcik and D. A. Koss, unpublished research.

List of Figures

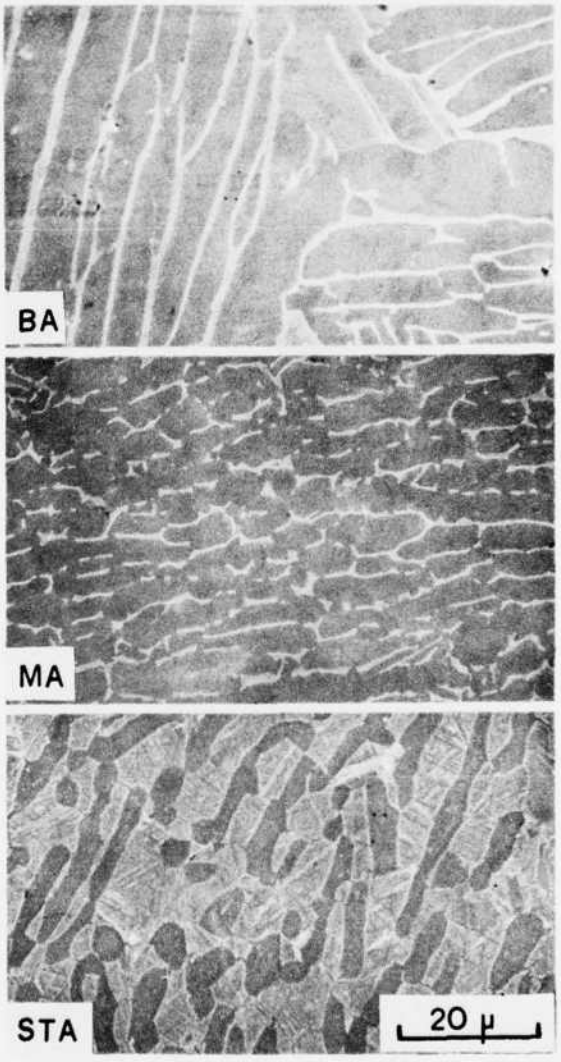


Fig. 1. Examples of the microstructures of the Ti-6Al-4V samples in the beta-annealed (BA), mill-annealed (MA), and solution-treat-and-aged (STA) conditions. Sections are perpendicular to the rolling direction. The hardness $R_c$ and yield strengths for the BA, MA, and STA conditions are: 35 and 896, 34 and 862, and 38 and 1007 MPa, respectively.

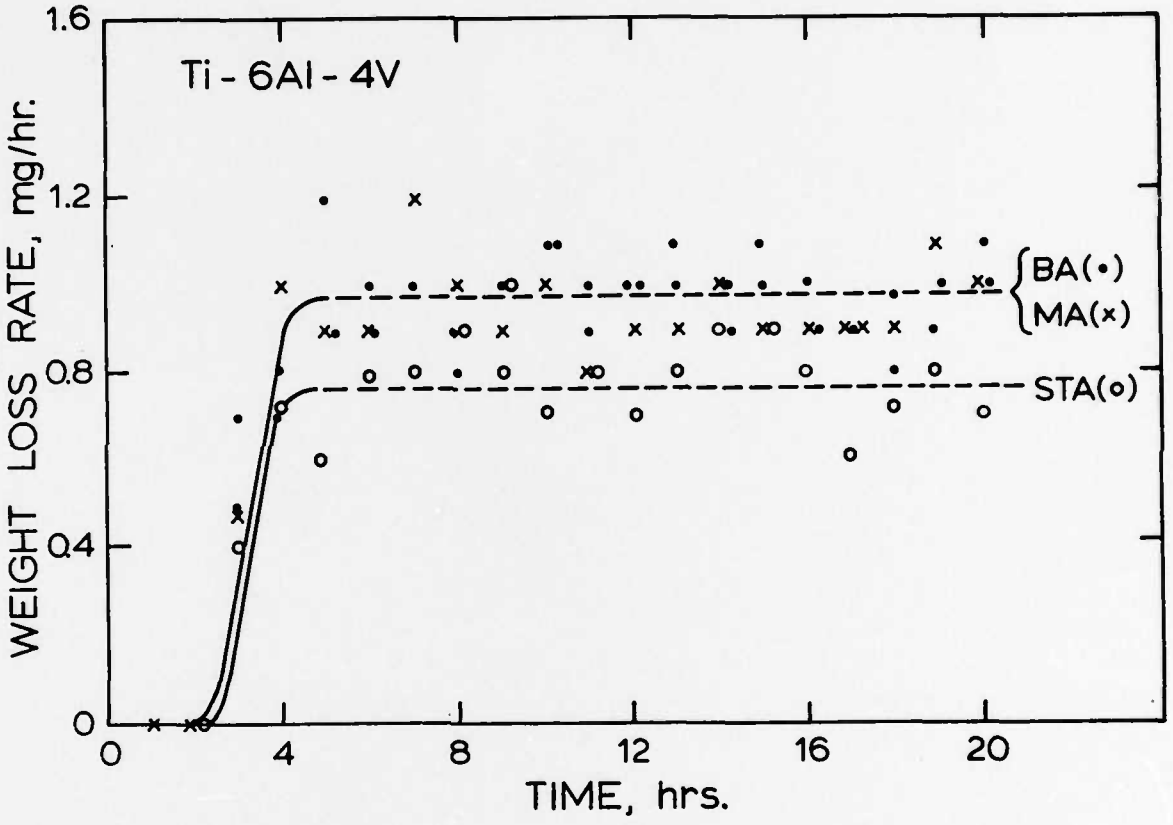


Fig. 2. The dependence of cavitation-induced erosion rate on exposure time for Ti-6Aℓ-4V in the beta-annealed (BA), mill-annealed (MA) and solution-treat-and-aged (STA) conditions. The dotted lines indicate the mean erosion rate between 4 and 14 hours for a given heat treatment.

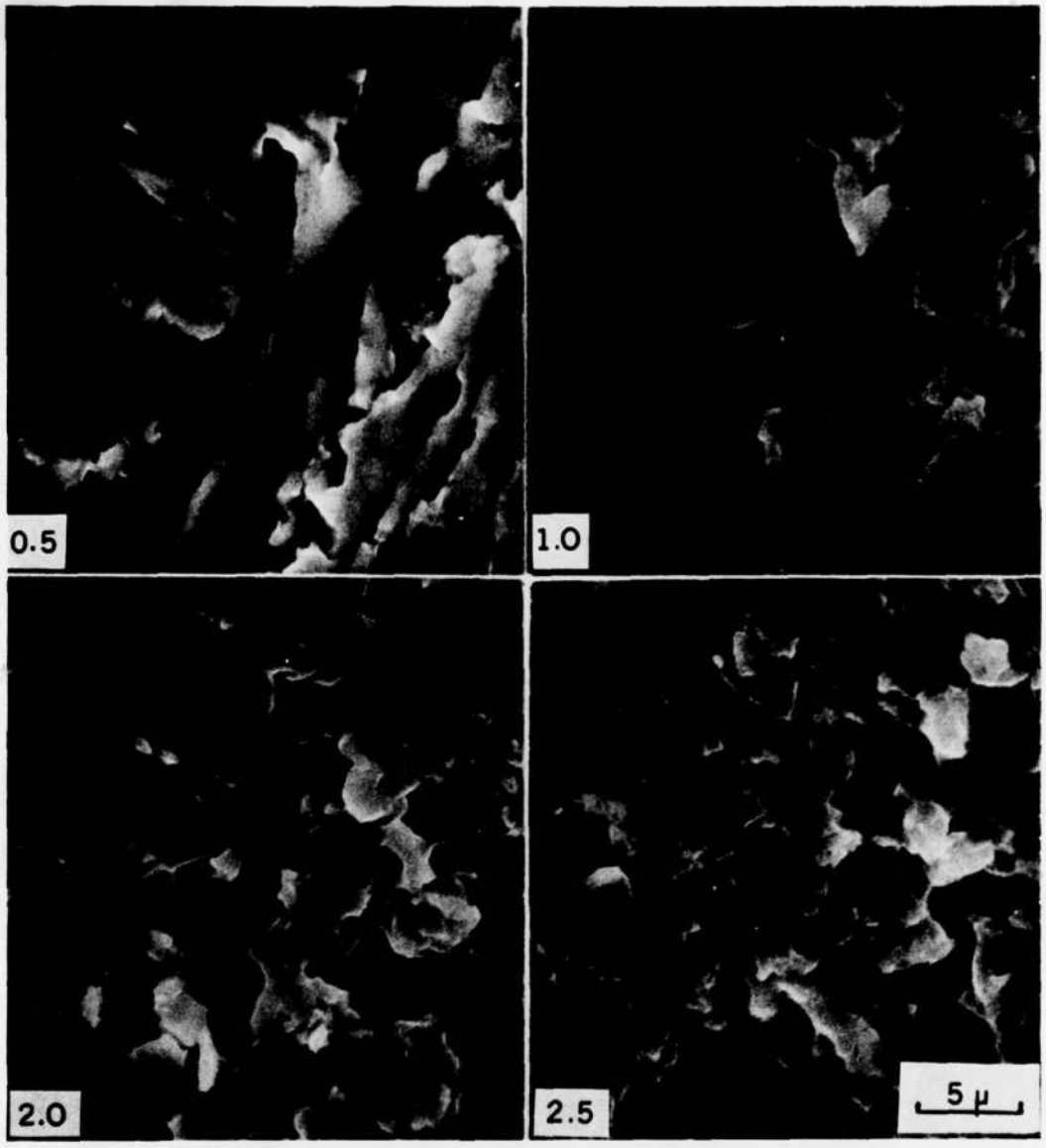


Fig. 3. Surface topography of an eroded beta-annealed sample showing the same area after 0.5, 1.0, 2.0, and 2.5 hours of exposure to cavitation. The letter S indicates the location of slip bands.

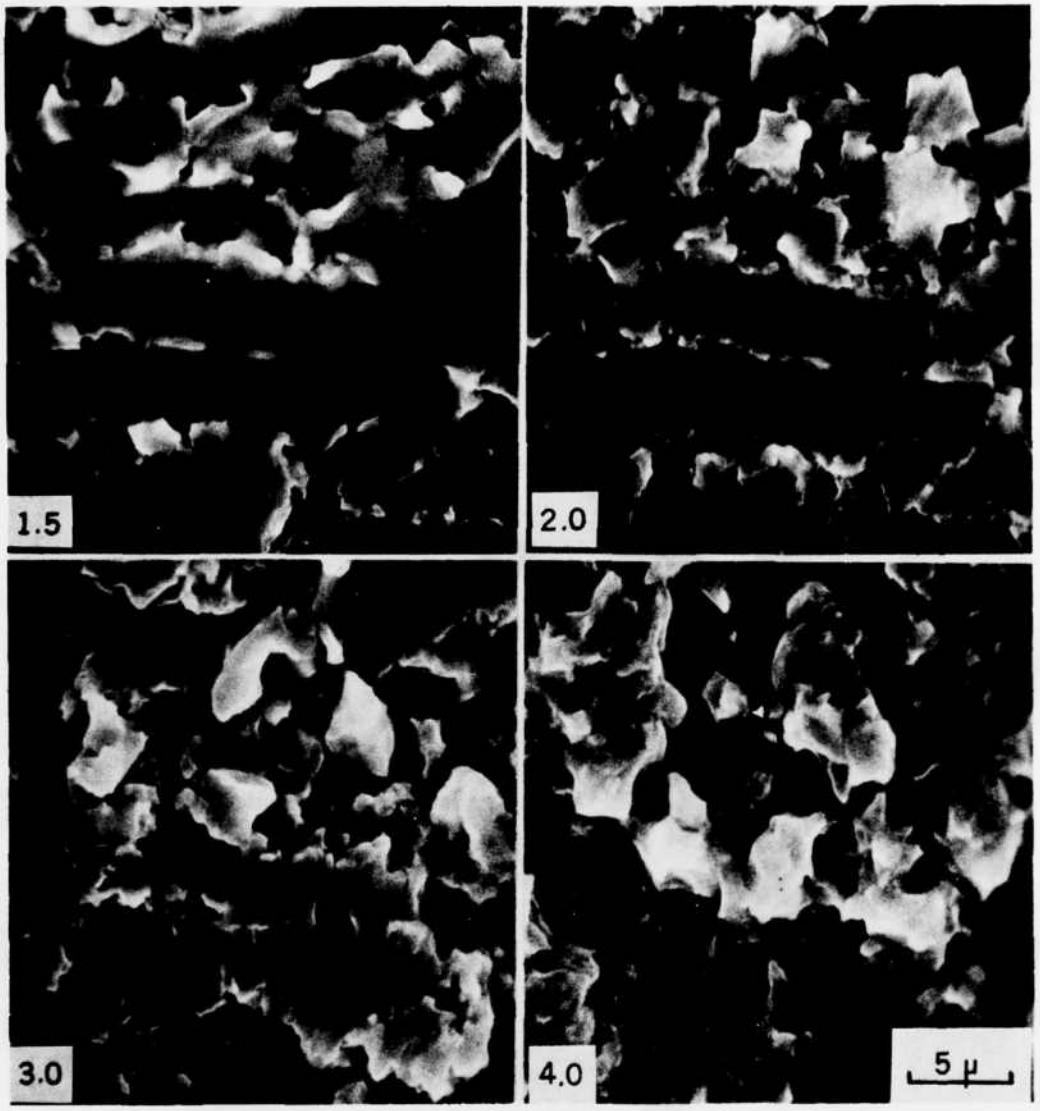


Fig. 4. Surface topography of an eroded mill-annealed sample showing the same area after 1.5, 2.0, 3.0, and 4.0 hours of exposure to cavitation.

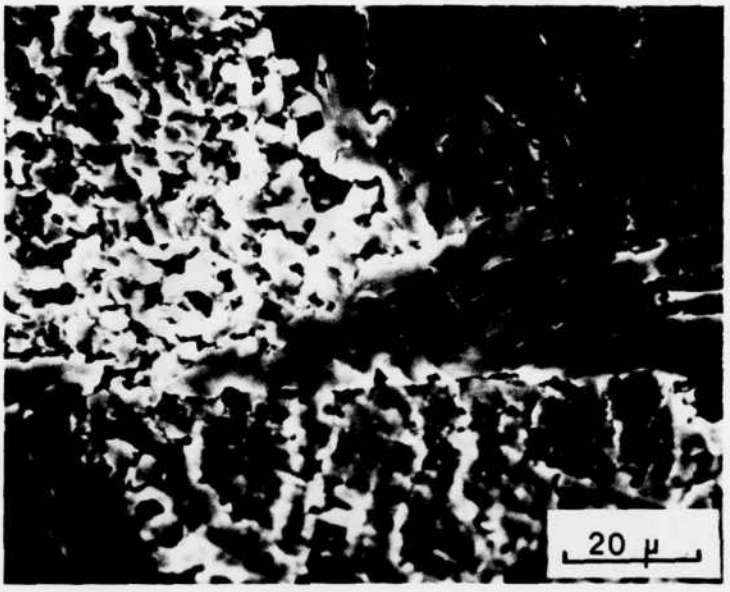


Fig. 5. Surface topography of a beta-annealed sample showing the dependence of the early stages of cavitation erosion on the Widmanstatten colony orientation after 2.0 hours exposure time.

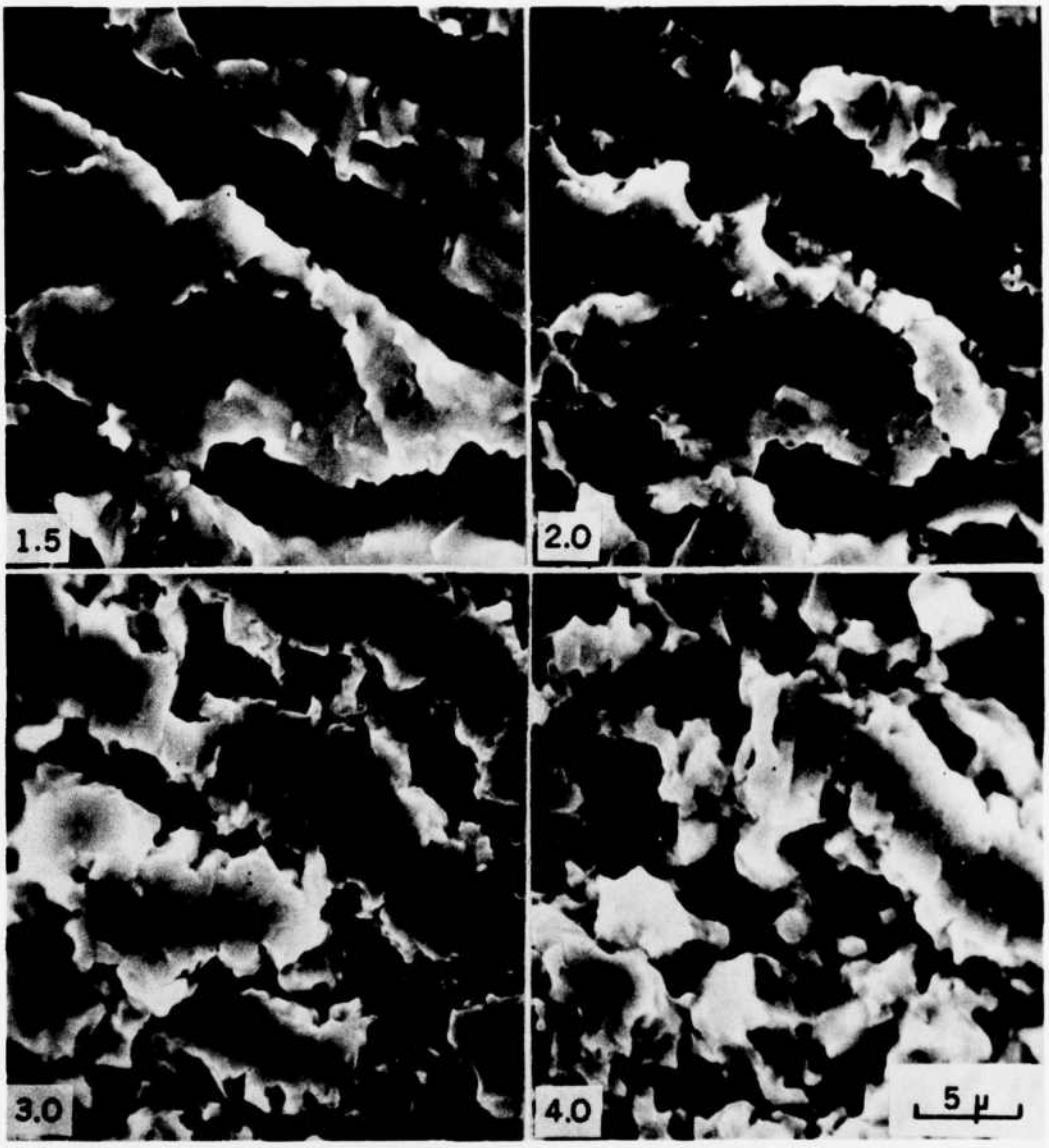


Fig. 6. Surface topography of an eroded solution-treat-and-aged sample showing the same area after 1.5, 2.0, 3.0, and 4.0 hours of exposure to cavitation.

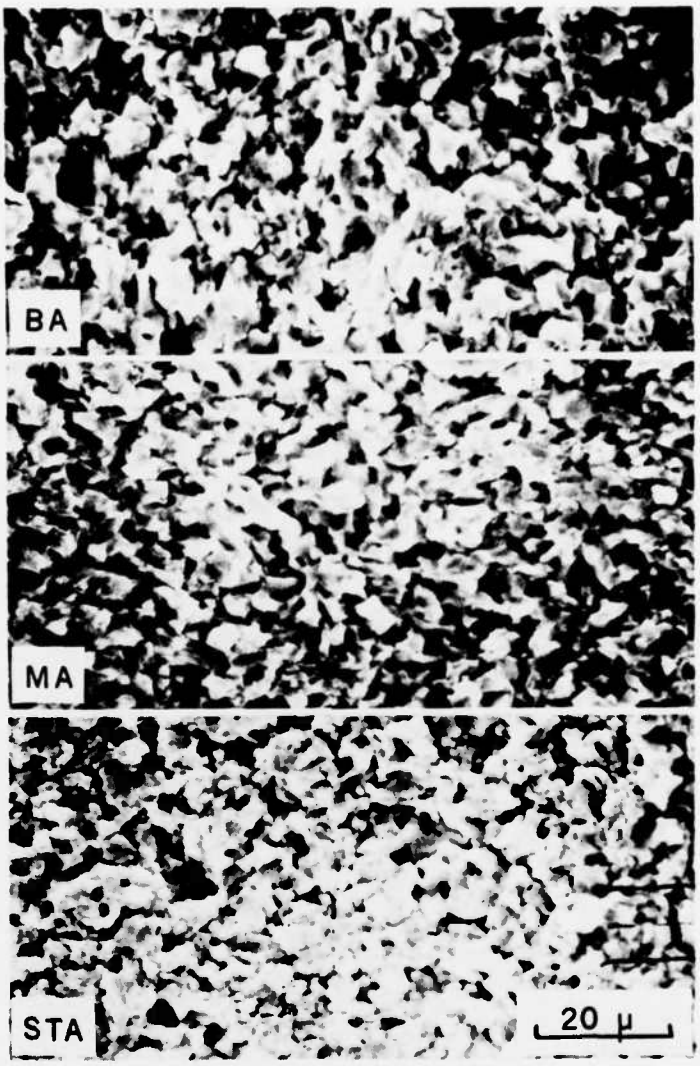


Fig. 7. Surface topographies of beta-annealed (BA), mill-annealed (MA), and solution-treat-and-aged (STA) samples after 14 hours of cavitation erosion.

SECURITY CLASSIFICATION OF THIS PAGE (When Data Entered)

## REPORT DOCUMENTATION PAGE

READ INSTRUCTIONS BEFORE COMPLETING FORM

1. REPORT NUMBER: No. 8
2. GOVT ACCESSION NO.
3. RECIPIENT'S CATALOG NUMBER: (9) Technical rept.

4. TITLE (and Subtitle): (6) Cavitation-Induced Erosion of Ti-6Al-4V.
5. TYPE OF REPORT & PERIOD COVERED: (14) TR-8
6. PERFORMING ORG. REPORT NUMBER

7. AUTHOR(s): (10) D. Essenmacher, M. F. Prezkop, D. E. Mikkola, D. A. Koss
8. CONTRACT OR GRANT NUMBER(s): (15) N00014-76-C-0037

9. PERFORMING ORGANIZATION NAME AND ADDRESS:
Dept. of Metallurgical Engineering
Michigan Technological University
Houghton, Michigan 49931

10. PROGRAM ELEMENT, PROJECT, TASK AREA & WORK UNIT NUMBERS

11. CONTROLLING OFFICE NAME AND ADDRESS:
Metallurgy Program, Office of Naval Research
800 North Quincy St.
Arlington, VA 22217

12. REPORT DATE: (11) Oct[illegible]77
13. NUMBER OF PAGES: (12) 20p.

14. MONITORING AGENCY NAME & ADDRESS (if different from Controlling Office)

15. SECURITY CLASS. (of this report): Unclassifed
15a. DECLASSIFICATION/DOWNGRADING SCHEDULE

16. DISTRIBUTION STATEMENT (of this Report)

Distribution of this document is un limited.

17. DISTRIBUTION STATEMENT (of the abstract entered in Block 20, if different from Report)

18. SUPPLEMENTARY NOTES

19. KEY WORDS (Continue on reverse side if necessary and identify by block number)

Erosion, Cavitation, Ti Alloy, Fracture

20. ABSTRACT (Continue on reverse side if necessary and identify by block number)

Cavitation-induced erosion has been examined in Ti-6Al-4V in the mill annealed, solution-treat-and-aged, and beta annealed conditions. Weight-loss data show only small differences between heat treatments with the solution-treat-and-aged microstructure exhibiting the lowest weight loss rates. Sequential micrographs of the same specimen area as a function of erosion time show that initially fracture occurs along the α-β interfaces and along crystallographic slip bands in the α-phase. The early stages of erosion are also dependent on

(cont'd)

DD FORM 1 JAN 73 1473 EDITION OF 1 NOV 65 IS OBSOLETE
S/N 0102-014-6601 |

SECURITY CLASSIFICATION OF THIS PAGE (When Data Entered)

402311 Jane

20. Abstract (cont'd)

the orientation of the Widmanstatten colonies in the beta annealed condition. These observations strongly suggest that fatigue fracture is important, at least in the early stages of the cavitation erosion process. Depression of the softer α-phase also occurs at short exposure times, and this leads to fracture and removal of the exposed phase; i.e., β or tempered martensite. However, examination of the eroded surfaces in the later stages where considerable material has been removed shows no evidence of the underlying microstructure, despite the distinct differences in the microstructures of the samples tested.


DAT
FILM